

Inverse Kinematics Analysis of the Three-Legged Reconfigurable Spherical Robot II

Natthaphon Bunathuek

Graduate School of Computer Science and Systems
Engineering
Kyushu Institute of Technology
Fukuoka, JAPAN
e-mail: q794034a@mail.kyutech.jp

Pudit Laksanacharoen

Mechanical and Aerospace Engineering Department
King Mongkut University of Technology
North Bangkok
Bangkok, THAILAND
e-mail: doctornoom@gmail.com

Abstract—The reconfigurable spherical robot called “RSR” is a transformable robot that store its three legs in the spherical shell. The RSR II is an ongoing work developed at King Mongkut’s University of Technology North Bangkok. At deployment, the robot can be transformed into a mobile form of dual interconnected hemispheres. Two legs are kept on one side of the hemisphere and one leg is on the other. Each leg is identical and has been designed with four degrees of freedom for good mobility. This paper represents the inverse kinematics analysis of one leg of the RSR II. The use of Denavit-Hartenberg (DH) method was illustrated to analyze for the forward kinematics of the leg. The solution of the closed form inverse kinematics of the leg was explained as well as the trajectory design for each leg.

Keywords- spherical robot, inverse kinematics

I. INTRODUCTION

Spherical robots have become more interested in many roboticist since its body can roll efficiently in various environment and can be easy in transportation and deployment. Nevertheless, the spherical body has its constraint; for example, the driving forces has to be driven from inside of the shell, or the body can be opened to become a wheeled or legged type robot.

Many researchers have been constructed various types of spherical shape robot with self driving from inner shell. First type of spherical robot consists of robots that include wheeled robot inside the shell. The shell is rolling by moving the wheel or some devices to propel force on the shell surface such as Bicchi et al [1], Hou [2], Kim [3].

Another type of spherical robots use the effect of inner pendulum. The center of mass of the spherical is deviated from its center by rotating the arm of the pendulum causing motion on the shell Salter [4], Gajbhiye [5]. A deformable spherical rolling robot using SMA actuators that achieves an eccentric center of mass by changing the shape of the spherical shell by Sugiyama et al [6].

Most of the previous work on spherical robot locomotion have been done on either the inner driving mechanism or the deformable shell’s surface. The authors have developed a method in which the robot in spherical shape can transform into a three-legged robot [7]-[10].

Previously, the RSR II has been designed and constructed but has no complete analytical inverse kinematic solution. This paper represents the inverse kinematics analysis

equation on each leg for design the trajectory of robot by using an ellipse mathematical equation.

Inverse kinematics problem is one of the important topics in robotic research. There are various types of method such as neural networks [11], closed form inverse kinematics [12]. This work uses a closed form analysis for the inverse kinematic analysis of the leg of RSR II.

II. BACKGROUND

The RSR II consists of two hemispherical shells and three legs kept inside the shell as shown in Fig. 1. The outer shells are made of fiberglass to strengthen its structure with a diameter of 350 mm.

For simplicity, all three legs have the same configuration. There are a total of 4 motors on each leg: 2 motors for shoulder/hip joint, 1 motor/degree of freedom for elbow, and 1 motor/degree of freedom for wrist joint.

Each leg is attached to the edge of hemispherical shell. The transformation process is driven by a motor at each joint. When fully transformed, the robot leg should be able to provide standing on ground. The robot has three omnidirectional passive wheels with a radius of 50 mm attached to the end of each leg.



Figure 1. Three-legged RSR

III. LEG KINEMATICS

We consider the kinematics of the leg in two parts; forward kinematics using Denavit-Hartenberg (DH) parameters and inverse kinematics in closed form.

A. Forward Kinematics

The robot has three identical leg kinematics. Each leg is a 4-DOF leg where all joints are revolute driven by 4 servomotors. The coordinate frame assignment are illustrated in Fig. 2. The DH parameters are listed in Table I. The coordinate frame $(x_0; y_0; z_0)$ to $(x_3; y_3; z_3)$ represent the local

coordinates frames at the four joints respectively, $(x_4; y_4; z_4)$ shows the local coordinate frame at the end effector.

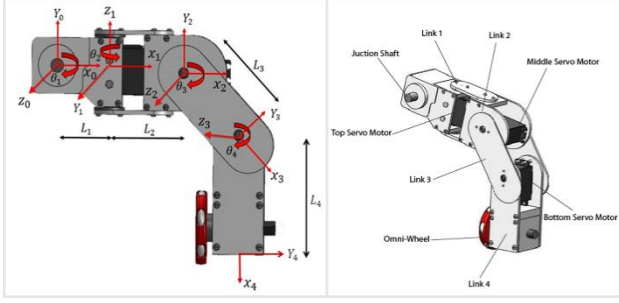


Figure 2. Leg kinematics

TABLE I. DH PARAMETERS

i	α_i	a_i	d_i	θ_i
1	$-\frac{\pi}{2}$	L_1	0	θ_1
2	$\frac{\pi}{2}$	L_2	0	θ_2
3	0	L_3	0	θ_3
4	0	L_4	0	θ_4

From the DH parameters, the transformation matrix from joint i to joint $i+1$ can be derived by:

$$T_{01} = \begin{bmatrix} \cos\theta_1 & 0 & -\sin\theta_1 & L_1 \cos\theta_1 \\ \sin\theta_1 & 0 & \cos\theta_1 & L_1 \sin\theta_1 \\ 0 & -1 & 0 & 0 \\ 0 & 0 & 0 & 1 \end{bmatrix} \quad (1)$$

$$T_{12} = \begin{bmatrix} \cos\theta_2 & 0 & \sin\theta_2 & L_2 \cos\theta_2 \\ \sin\theta_2 & 0 & -\cos\theta_2 & L_2 \sin\theta_2 \\ 0 & 1 & 0 & 0 \\ 0 & 0 & 0 & 1 \end{bmatrix} \quad (2)$$

$$T_{23} = \begin{bmatrix} \cos\theta_3 & -\sin\theta_3 & 0 & L_3 \cos\theta_3 \\ \sin\theta_3 & \cos\theta_3 & 0 & L_3 \sin\theta_3 \\ 0 & 0 & 1 & 0 \\ 0 & 0 & 0 & 1 \end{bmatrix} \quad (3)$$

$$T_{34} = \begin{bmatrix} \cos\theta_4 & -\sin\theta_4 & 0 & L_4 \cos\theta_4 \\ \sin\theta_4 & \cos\theta_4 & 0 & L_4 \sin\theta_4 \\ 0 & 0 & 1 & 0 \\ 0 & 0 & 0 & 1 \end{bmatrix} \quad (4)$$

$$T_{04} = T_{01}T_{12}T_{23}T_{34} \quad (5)$$

$$T_{04} = \begin{bmatrix} n_x & o_x & a_x & p_x \\ n_y & o_y & a_y & p_y \\ n_z & o_z & a_z & p_z \\ 0 & 0 & 0 & 1 \end{bmatrix} \quad (6)$$

$$n_x = -C_4(S_1S_3 - C_1C_2C_3) - S_4(S_1C_3 + C_1C_2C_3) \quad (7)$$

$$n_y = -C_4(C_1S_3 + S_1C_2C_3) + S_4(C_1C_3 + S_1C_2S_3) \quad (8)$$

$$n_z = S_2S_3S_4 - S_2C_3C_4 \quad (9)$$

$$o_x = S_4(S_1S_3 - C_1C_2C_3) - C_4(S_1C_3 + C_1C_2S_3) \quad (10)$$

$$o_y = C_4(C_1C_3 - S_1C_2S_3) - S_4(C_1S_3 + S_1C_2C_3) \quad (11)$$

$$o_z = S_2C_3S_4 + S_2S_3C_4 \quad (12)$$

$$a_x = C_1S_2 \quad (13)$$

$$a_y = S_1S_2 \quad (14)$$

$$a_z = C_2 \quad (15)$$

where $p_x; p_y; p_z$ are the global coordinates of the end effector shown below:

$$p_x = L_1C_1 - L_4C_4(S_1S_3 - C_1C_2C_3) - L_4S_4(S_1C_3 + C_1C_2C_3) + L_2C_1C_2 - L_3S_1S_3 + L_3C_1C_2C_3 \quad (16)$$

$$p_y = L_1S_1 + L_4C_4(C_1S_3 + S_1C_2C_3) + L_4S_4(C_1C_3 - S_1C_2S_3) + L_2S_1C_2 + L_3C_1S_3 + L_3S_1C_2C_3 \quad (17)$$

$$p_z = L_4S_2S_3S_4 - L_3S_2C_3 - L_4S_2C_3C_4 - L_2S_2 \quad (18)$$

where $C_i = \cos \theta_i, S_i = \sin \theta_i, i = 1, 2, 3, 4$

B. Inverse Kinematics

The forward kinematics equations are nonlinear. It is clearly that the inverse kinematics solution is difficult to solve. From equation (7) - (18), there will be many solutions of the equations.

Therefore, we use some technique to reduce those many solutions by defining some assumption for the problem. This paper uses the fixed orientation with the XYZ coordinate system as shown in Fig. 3.

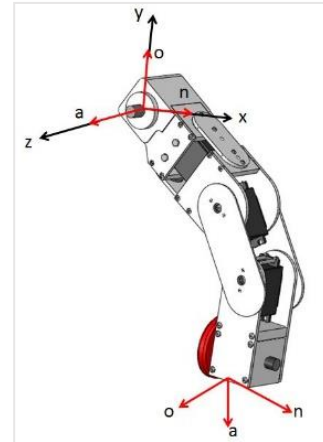


Figure 3. Leg orientation

Fig. 3 represents an end of effector orientation relative to the base coordinate system. a is the unit vector that has direction toward the object. o has its direction following with the end effector and vector n is the normal vector of a and o following by the right hand rule.

From equation (13) and (14) we can solve for θ_1 :

$$\theta_1 = a \tan 2[a_y, a_x] \quad (19)$$

Then multiplying equation (6) on both sides with transformation matrix T_{01}^{-1} we get

$$T_{01}^{-1}T_{01}T_{12}T_{23}T_{34} = T_{01}^{-1} \begin{bmatrix} n_x & o_x & a_x & p_x \\ n_y & o_y & a_y & p_y \\ n_z & o_z & a_z & p_z \\ 0 & 0 & 0 & 1 \end{bmatrix} \quad (20)$$

We can rewrite the equation as shown below

$$[A, B, C, D] = [E, F, G, H] \quad (21)$$

where

$$A = \begin{bmatrix} C_2C_3C_4 - C_2S_3S_4 \\ S_2C_3C_4 - S_2S_3S_4 \\ C_3S_4 + S_3C_4 \\ 0 \end{bmatrix}, B = \begin{bmatrix} -C_2C_3S_4 - C_2S_3C_4 \\ -S_2C_3S_4 - S_2S_3C_4 \\ C_3C_4 - S_3S_4 \\ 0 \end{bmatrix} \quad (22)$$

$$C = \begin{bmatrix} S_2 \\ -C_2 \\ 0 \\ 0 \end{bmatrix}, B = \begin{bmatrix} L_2C_2 + L_3C_2C_3 + L_4C_2C_3C_4 - L_4C_2S_3S_4 \\ L_2S_2 + L_3S_2C_3 + L_4S_2C_3C_4 - L_4S_2S_3S_4 \\ L_3S_3 + L_4C_3S_4 + L_4S_3C_4 \\ 1 \end{bmatrix} \quad (23)$$

$$E = \begin{bmatrix} n_xC_1 + n_yS_1 \\ -n_z \\ n_yC_1 - n_xS_1 \\ 0 \end{bmatrix}, F = \begin{bmatrix} o_xC_1 + o_yS_1 \\ -o_z \\ o_yC_1 - o_xS_1 \\ 0 \end{bmatrix} \quad (24)$$

$$G = \begin{bmatrix} a_xC_1 + a_yS_1 \\ -a_z \\ a_yC_1 - a_xS_1 \\ 0 \end{bmatrix}, H = \begin{bmatrix} p_xC_1 - L_1 + p_yS_1 \\ -p_z \\ p_yC_1 - p_xS_1 \\ 1 \end{bmatrix} \quad (25)$$

Consider

$$p_xC_1 + p_yS_1 - L_1 = C_2(L_2 + L_3C_3 + L_4C_3C_4 - L_4S_3S_4) \quad (26)$$

$$-p_z = S_2(L_2 + L_3C_3 + L_4C_3C_4 - L_4S_3S_4) \quad (27)$$

$$p_yC_1 - p_xS_1 = L_3S_3 + L_4C_3S_4 + L_4S_3C_4 \quad (28)$$

From (27) and (28) can solve for θ_2

$$\theta_2 = a \tan \left[\frac{-p_z}{p_xC_1 + p_yS_1 - L_1} \right] \quad (29)$$

In some cases, when we multiply transformation matrix $T_{12}^{-1}T_{01}^{-1}$ on both sides of the equation (20) we will get

$$T_{12}^{-1}T_{01}^{-1}T_{01}T_{12}T_{23}T_{34} = T_{12}^{-1}T_{01}^{-1} \begin{bmatrix} n_x & o_x & a_x & p_x \\ n_y & o_y & a_y & p_y \\ n_z & o_z & a_z & p_z \\ 0 & 0 & 0 & 1 \end{bmatrix} \quad (30)$$

$$T_{23}T_{34} = T_{12}^{-1}T_{01}^{-1} \begin{bmatrix} n_x & o_x & a_x & p_x \\ n_y & o_y & a_y & p_y \\ n_z & o_z & a_z & p_z \\ 0 & 0 & 0 & 1 \end{bmatrix} \quad (31)$$

$$[I, K, J, L] = [M, N, O, P] \quad (32)$$

$$I = \begin{bmatrix} C_3C_4 - S_3S_4 \\ C_3S_4 + S_3C_4 \\ 0 \\ 0 \end{bmatrix}, J = \begin{bmatrix} -C_3S_4 - S_3C_4 \\ C_3C_4 - S_3S_4 \\ 0 \\ 0 \end{bmatrix} \quad (33)$$

$$K = \begin{bmatrix} 0 \\ 0 \\ 1 \\ 0 \end{bmatrix}, L = \begin{bmatrix} L_3C_3 + L_4C_3C_4 - L_4S_3S_4 \\ L_3S_3 + L_4C_3S_4 + L_4S_3C_4 \\ 0 \\ 1 \end{bmatrix} \quad (34)$$

$$M = \begin{bmatrix} n_xC_1C_2 - n_zS_2 + n_yS_1C_2 \\ n_yC_1 - n_xS_1 \\ n_zC_2 + n_xC_1S_2 + n_yS_1S_2 \\ 0 \end{bmatrix}, N = \begin{bmatrix} o_xC_1C_2 - o_zS_2 + o_yS_1C_2 \\ o_yC_1 - o_xS_1 \\ o_zC_2 + o_xC_1S_2 + o_yS_1S_2 \\ 0 \end{bmatrix} \quad (35)$$

$$O = \begin{bmatrix} a_xC_1C_2 - a_zS_2 + a_yS_1C_2 \\ a_yC_1 - a_xS_1 \\ a_zC_2 + a_xC_1S_2 + a_yS_1S_2 \\ 0 \end{bmatrix}, N = \begin{bmatrix} p_xC_1C_2 - L_1C_2 - p_zS_2 - L_2 + p_yS_1C_2 \\ p_yC_1 - p_xS_1 \\ p_zC_2 - L_1S_2 + p_xC_1S_2 + p_yS_1S_2 \\ 1 \end{bmatrix} \quad (36)$$

Consider factor of equation (32) then

$$L_3C_3 + L_4C_3C_4 - L_4S_3S_4 = p_xC_1C_2 - L_1C_2 - p_zS_2 - L_2 + p_yS_1C_2 \quad (37)$$

From equation (37)² we get

$$(L_3C_3 + L_4C_3C_4 - L_4S_3S_4)^2 = (p_xC_1C_2 - L_1C_2 - p_zS_2 - L_2 + p_yS_1C_2)^2 \quad (38)$$

From equation (28)2 we get

$$(L_3S_3 + L_4C_3S_4 + L_4S_3C_4)^2 = (p_yC_1 - p_xS_1)^2 \quad (39)$$

Summing the equation (38) and (39), we will get

$$L_3^2 + L_4^2 + 2L_3L_4 \cos \theta_4 = (p_xC_1C_2 - L_1C_2 - p_zS_2 - L_2 + p_yS_1C_2)^2 + (p_yC_1 - p_xS_1)^2 \quad (40)$$

Define

$$C = (p_xC_1C_2 - L_1C_2 - p_zS_2 - L_2 + p_yS_1C_2)^2 + (p_yC_1 - p_xS_1)^2 \quad (41)$$

Rewrite

$$L_3^2 + L_4^2 + 2L_3L_4 \cos\theta_4 = C \quad (42)$$

We can now solve for θ_3

$$\theta_4 = \cos^{-1} \left[\frac{C - L_3^2 - L_4^2}{2L_3L_4} \right] \quad (43)$$

From the equation (37) can reformation to get

$$p_y C_1 - p_x S_1 = (L_3 + L_4 C_4) S_3 + (L_4 S_4) C_3 \quad (44)$$

From trigonometry

$$a \sin \theta + b \cos \theta = c$$

When

$$a = L_3 + L_4 C_4, \quad b = L_4 S_4 \quad \text{and} \quad c = p_y C_1 - p_x S_1$$

We can now solve for θ_4

$$\theta_3 = a \tan 2 \left[\sqrt{a^2 + b^2 - c^2} + ac, -a \sqrt{a^2 + b^2 - c^2} + bc \right] \quad (45)$$

IV. TRAJECTORY DESIGN

The motion of the two front legs of the robot has been designed to be able to walk like butterfly walking pattern.

For the motion of left leg and right leg, we will be using ellipse equation (46), (47) respectively

$$\begin{cases} x = 80 + 80 \sin \phi \\ y = 140 \cos \phi \end{cases} \quad (46)$$

$$\begin{cases} x = 80 + 80 \sin \phi \\ z = -10 + 140 \cos \phi \end{cases} \quad (47)$$

Fig. 4 and Fig. 5 shows the trajectory design of the left and right leg respectively. The trajectory of the left and right leg are mirroring during the walking pattern.

For the back leg in equation (48)

$$\begin{cases} x = 150 + 50 \sin \phi \\ y = 50 + 100 \cos \phi \end{cases} \quad (48)$$

The back leg trajectory gives the forward propulsion of the robot as shown in Fig. 6.

The joint angle function on each link will be a function of time as a polynomial order 3 as shown in equation (49)

$$q(t) = a_0 + a_1 t + a_2 t^2 + a_3 t^3 \quad (49)$$

with initial conditions are

$$q(0) = \theta_{start}, \quad q(t_g) = \theta_{goal}, \quad \dot{q}(0) = 0 \quad \text{and} \quad \dot{q}(t_g) = 0$$

Solving for coefficients of the polynomial from initial conditions $\theta_{start} = 0$; $\theta_{goal} = \pi$; $t_g = 0$ sec, we get

Therefore the $q(t)$ is a function as

$$q(t) = 0.0942t^2 - 0.00628t^3 \quad (50)$$

V. EXPERIMENTAL RESULTS

For statically stable, it is required that at least three legs are on the ground while moving. Since this robot II has three legs, there must be some arbitrary contact while some legs are off the ground. This work proposed the three legs walking inspired by the butterfly walking concept. While a pair of front legs lift off the ground, the lowest part of its hemisphere helps support for stable walking until both front legs touch the ground to push and lift its body for moving forward. One back leg pushed to drive the robot moving forward.

Results has been verified in MATLAB in the trajectory planning for leg moving in butterfly walking concept as shown in Fig. 7. The trajectory of three legs are shown in Fig. 8.

In forward motion, the two front legs trajectory give swing motion correlating with the graph shown in Fig. 9 and 10. The back leg trajectory gives pushing force as shown in Fig. 11.

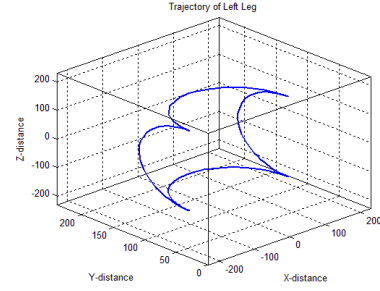


Figure 4. Trajectory design of left leg

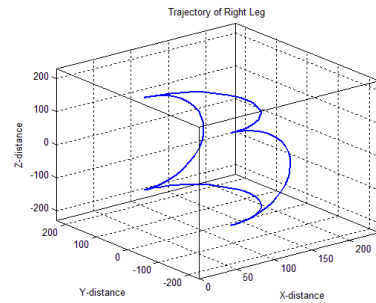


Figure 5. Trajectory design of right leg

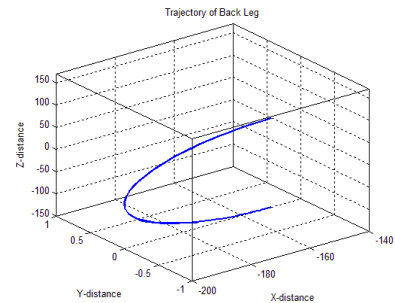


Figure 6. Trajectory design of back leg

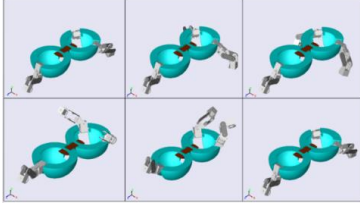


Figure 7. Simulation results in butterfly walking concept

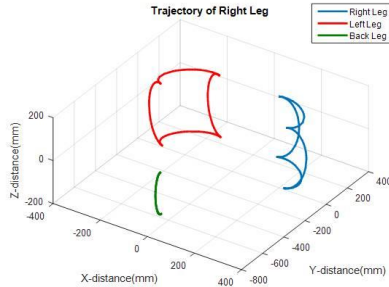


Figure 8. Trajectory of three legs

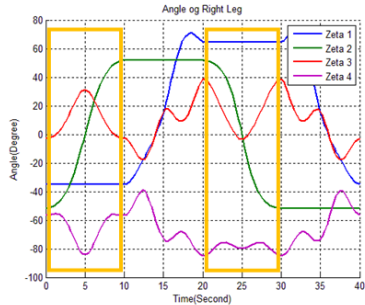


Figure 9. Joint angle for right leg

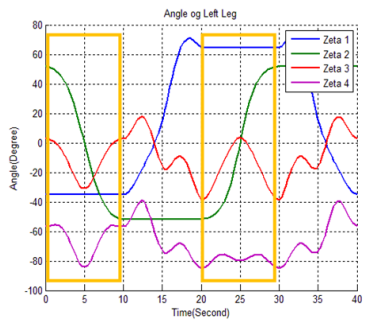


Figure 10. Joint angle for left leg

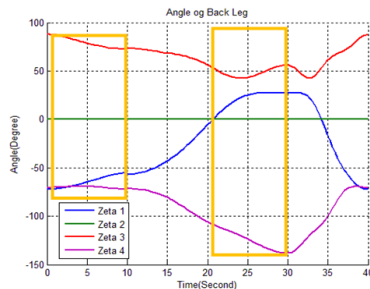


Figure 11. Joint angle for back leg

VI. CONCLUSIONS

An analytical solution of the inverse kinematic problem for reconfigurable spherical robot II has been proposed. The solution is given in a closed form. Thus analysis for perfect answer of inverse kinematics equation as presented in this work can make three legs reconfigurable spherical robot moving in the concept of butterfly walking pattern. In future work, we will use this concept to apply to the actual reconfigurable spherical robot II walking.

REFERENCES

- [1] A. Bicchi, A. Balluchi, D. Prattichizzo, and A. Gorelli, "Introducing the sphericle: an experimental testbed for research and teaching in nonholonomy," *Proceedings of International Conference on Robotics and Automation*, vol. 3, pp. 2620–2625, 1997.
- [2] K. Hou, H. Sun, Q. Jia, and Y. Zhang, "An autonomous positioning and navigation system for spherical mobile robot," *Procedia Engineering*, vol. 29, pp. 2556 – 2561, 2012.
- [3] Y.-M. Kim, S.-S. Ahn, and Y.-J. Lee, "Kisbot: New spherical robot with arms," in *Proceedings of the 10th WSEAS International Conference on Robotics, Control and Manufacturing Technology*, ser. ROCOM'10. Stevens Point, Wisconsin, USA: World Scientific and Engineering Academy and Society (WSEAS), 2010, pp. 63–67.
- [4] T. Salter, F. Michaud, and D. Letourneau, "Roball interacting with children," in *Proceedings of the 4th ACM/IEEE International Conference on Human Robot Interaction*, ser. HRI '09. New York, NY, USA: ACM, 2009, pp. 209–210. S. Gajbhiye and R. N. Banavar, "The euler-poincar equations for a spherical robot actuated by a pendulum," *IFAC Proceedings Volumes*, vol. 45, no. 19, pp. 72 – 77, 2012.
- [5] S. Gajbhiye and R. N. Banavar, "The euler-poincar equations for a spherical robot actuated by a pendulum," *IFAC Proceedings Volumes*, vol. 45, no. 19, pp. 72 – 77, 2012.
- [6] Y. Sugiyama and S. Hirai, "Crawling and jumping by a deformable robot," *The International Journal of Robotics Research*, vol. 25, no. 5-6, pp. 603–620, 2006.
- [7] N. Chadil, M. Phadoongsidhi, K. Suwannasit, P. Manoonpong, and P. Laksanacharoen, "A reconfigurable spherical robot," in *2011 IEEE International Conference on Robotics and Automation (ICRA2011)*, Shanghai, China, May 9-13 2011.
- [8] P. Jearanaisilawong, S. Laksanacharoen, V. Piriya Wong, and K. Swatdipisal, "Design of a three-legged reconfigurable spherical shape robot," in *2009 IEEE/ASME International Conference on Advanced Intelligent Mechatronics(AIM2009)*, Suntec Convention and Exhibition Center, Singapore, July 14-16 2009.
- [9] P. Jearanaisilawong and S. Laksanacharoen, "Dynamic simulation of a reconfigurable spherical robot," in *Proceedings of the 2008 IEEE International Conference on Robotics and Biomimetics(Robio2008)*, Bangkok, Thailand, February 21-26 2009.
- [10] J. Q. Gan and E. M. R. Eimei Oyama, "A complete analytical solution to the inverse kinematics of the pioneer 2 robotic arm," *Robotics*, vol. 23, pp. 123–129, 2005.
- [11] S. Tejomurtula and S. Kak, "Inverse kinematics in robotics using neural networks," *Information Sciences*, vol. 116, pp. 147–164, 1999.
- [12] N. Kofinas, E. Orfanoudakis, and M. G. Lagoudakis, "Complete analytical forward and inverse kinematics for the nao humanoid robot," *Journal of Intelligent & Robotic Systems*, vol. 77, no. 2, pp. 251–264, 2015.